

Side Lobe Reduction Using Centroid and Flatness in Passive Cavitation Imaging

Mok Kun Jeong¹ and Sung Jae Kwon²

¹Department of Electronic Engineering

²Division of Human IT Convergence Engineering

Daejin University

Pocheon, Republic of Korea

jmk@daejin.ac.kr

Min Joo Choi

Department of Medicine

School of Medicine

Jeju National University

Jeju, Republic of Korea

Abstract—Cavitation bubbles generated by high-intensity focused ultrasound strongly collapse and emit ultrasound waves. Since passive cavitation imaging can be performed using only receive focusing, side lobes appear over a wide area of an image. The delay and sum beamforming technique used to construct passive cavitation images cannot effectively image the cavitation occurrence time and spatial distribution because a small cavitation signal is buried in the side lobe of a large cavitation signal when there are a large number of cavitation bubbles. The ultrasound wave emitted when the cavitation bubble collapses is a short duration pulse. After compensating for the focusing delay, the signals due to the main lobe (at the imaging point) received at each element of the transducer array are similar in magnitude, but those due to the side lobes (other than the imaging point) is significant only at some elements of the array. Using this characteristic of the received channel data, we propose both centroid and flatness as metrics to evaluate the effect of the main and side lobes at imaging points. If the centroid of the signal magnitude distribution of the entire receiving channel is positioned at the center of the array, the signal is considered to be due to the main lobe. However, if the centroid is computed to be located near both ends of the array, the signal is considered to be due to the side lobes. If the signals are found to be due to the side lobes in passive cavitation imaging, the pixel brightness is reduced by weighting using the centroid and flatness metrics. We computed the centroid and flatness metrics using computer simulation and experimental data, and confirmed the suppression of side lobes by multiplying the image by a weight using the centroid and flatness. The proposed method makes it easier to observe cavitation by effectively removing side lobes from passive cavitation images when the number of cavitation bubbles is not large.

Keywords—centroid; flatness; passive cavitation imaging; ultrasound; weighting

I. INTRODUCTION

Passive cavitation can occur when a high-intensity focused ultrasound (HIFU) or shock wave is illuminated on a medium. The ultrasound wave induces a change in pressure as it compresses and expands the medium during its propagation, generating bubbles mainly by negative pressure. These generated bubbles suddenly shrink in an inertial manner and

collapse at some time instant, causing passive ultrasonic cavitation. Ultrasonic cavitation due to bubble collapse creates secondary ultrasonic or shock waves. Since secondary ultrasonic waves generated in a series of processes such as bubble generation due to HIFU, dynamic behavior of bubbles, and inertial collapse cause various ultrasonic effects such as cell and stone destruction, it is very important to monitor and track ultrasonic waves generated due to ultrasonic cavitation [1]–[6].

Ultrasonic waves generated due to passive cavitation take the form of a short pulse. Signals received at individual elements of an array transducer arrive at different times depending on the distance from cavitation bubbles. In passive cavitation imaging, transmit focusing is not possible, and thus the axial resolution cannot be achieved by time gating. Applying receive focusing to increase resolution aligns the received channel signals from an imaging point of interest as if they have arrived at the same time. However, the received channel signals from elsewhere do not align in time even after the receive focusing. These nonaligned signals act as side lobes in image, reduce contrast, and make it difficult to observe passive cavitation. In this paper, we propose using centroid and flatness as two parameters that represent the amplitude distribution of the received channel data

II. THEORY

In an ultrasound receive focusing system, the received channel data are aligned by applying focusing delays and thereby compensating for different propagation distances. Fig. 1(a) shows the waveform of the channel data after applying focusing delays to ultrasonic echoes returned from an imaging point of interest. The amplitude of the channel data across the channels is uniform because the echoes are received at the same time across the channels. Fig. 1(b) shows the case of echoes returned from elsewhere. Since ultrasonic pulse echoes are usually short in duration, the signal amplitude of all the receive channels is not uniform. The distribution of signal amplitude across the receive channels is different for different incident angles, depending on whether the echoes return from an imaging point of interest or not.

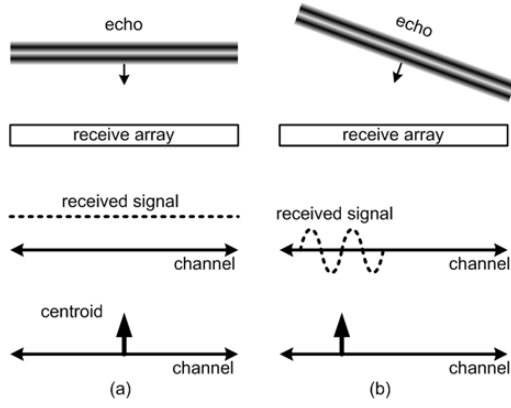


Fig. 1. Waveforms of echoes across receiving array: (a) from imaging point and (b) from other than imaging point.

We propose centroid as a parameter that represents the signal amplitude distribution of the received channel data, which is defined as follows:

$$Centroid(x, z) = \frac{\sum_{ch=1}^{N_{ch}} ch \cdot |r(ch)_{xz}|}{\sum_{ch=1}^{N_{ch}} |r(ch)_{xz}|}, \quad (1)$$

where N_{ch} is the total number of the receive channels, $r(ch)_{xz}$ is the received signal at (x, z) pixel on channel ch , and its absolute value $|r(ch)_{xz}|$ is used. In Fig. 1(a), since the signal amplitude of all the channels is the same, the centroid is at the center channel. For the case of side lobe signal as in Fig. 1(b), the centroid is located away from the center channel. Thus, as the centroid gets close to the center channel, the likelihood that the echoes have originated from an imaging point of interest increases. When suppressing side lobes using the centroid, the centroid is converted into a weighting value.

Fig. 2 shows an example of weight values as a function of the centroid in a 64 channel system. The solid and dashed lines represent a triangular weight and another weight given by the 4th power of the Hamming window, respectively. The centroid weighting is normalized such that the weight is 1 when the centroid is at the center channel and 0 when at both ends of the channels. Accordingly, a weight of 1 indicates that the echo is the main lobe signal returned from an imaging point of interest, and a weight less than 1 indicates that the echo is the side lobe signal returned from elsewhere.

The flatness is computed from the variance of all the receive channel data. As it gets close to 1, the signal magnitude across the receive channels gets more similar. The flatness at an imaging point is defined as follows:

$$Flatness(x, z) = 1 - \frac{\text{var}(r(ch)_{xz})}{\max[\text{var}(r(ch)_{xz})]}, \quad (2)$$

where $\text{var}(r(ch)_{xz})$ is the variance of all the receive channel data at an imaging point (x, z) . The variance at all pixels of an image frame is computed and normalized to the largest variance so that $0 \leq Flatness(x, z) \leq 1$.

We can suppress side lobes by multiplying a pixel value by the centroid weight and the flatness at each pixel of ultrasonic image, as follows:

$$Pixel(x, z)_{filtered} = Flatness(x, z) \cdot centroid_weighting(x, z) \cdot Pixel(x, z), \quad (3)$$

where $Pixel(x, z)$ is the input pixel value and $Pixel(x, z)_{filtered}$ is the output pixel value. Since in passive cavitation imaging the bubble collapse can be modeled as a point source and the ultrasonic signal is a short pulse, the centroid and flatness can effectively be used to suppress side lobes.

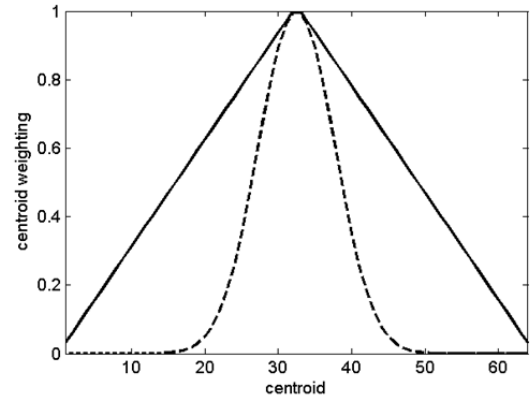


Fig. 2. Centroid weighting as a function of centroid in a 64 channel imaging system: a triangular weight (solid) and a weight given by the 4th power of the Hamming window (dashed).

III. COMPUTER SIMULATION

Passive cavitation was simulated using ultrasonic waves generated due to cavitation. The ultrasonic signal generated due to cavitation was modeled as a point source at a depth of 30 mm, and was assumed to take the form of a pulse with a center frequency of 5 MHz. The RF signal was received by a 5 MHz, 64 element linear array transducer with a pitch of 0.6 mm, and was sampled at 80 MHz.

In Fig. 3, (a) is the delay and sum (DAS) image of a single cavitation drawn in linear scale, where the side lobes take the form of an X shape over a large area, (b) is a weight profile given by the 4th power of the Hamming window, in which the weight values are small in the region shaped like X where side lobes are present, (c) is the flatness whose value is large at imaging points around the region of passive cavitation, and (d) is the result of multiplying together the centroid weighting and the flatness.

Fig. 4 compares the magnitude distribution of the channel data for the case of Fig. 3(a). The signal magnitude distribution in the cavitation region (solid) is quite uniform across the channels, with the centroid and weighting being 29.9 and 0.76, respectively. The signal magnitude distribution in the side lobe region (dotted) looks like a Gaussian distribution whose mean is centered at the center channel, with the centroid and weighting being 31.4 and 0.48, respectively, while that in the other region (dashed) deviates significantly from the center channel, with the centroid and weighting being 41.1 and 0.1983, respectively

Fig. 5 shows the weighted DAS image, which is logarithmically compressed over a range of 40 dB to be able to observe side lobes, where the side lobe region is seen to be reduced.

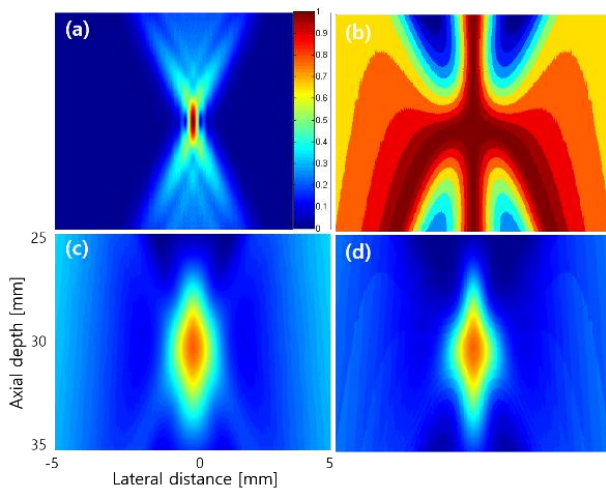


Fig. 3. Pseudocolor representation: (a) point-like bubble image, (b) centroid weighting, (c) flatness, and (d) multiplication of centroid weighting and flatness.

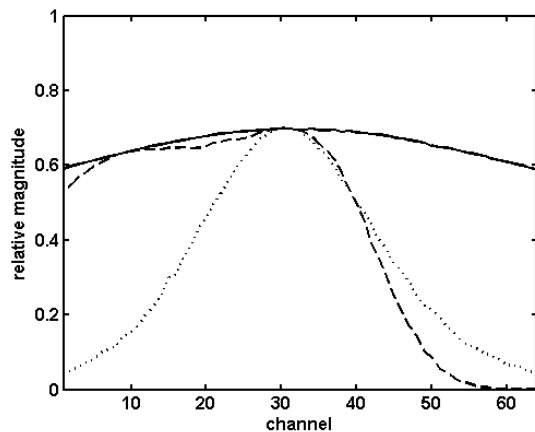


Fig. 4. Comparison of the signal magnitude distribution in receive channels from the cavitation region (solid), side lobe region (dotted), and other region (dashed).

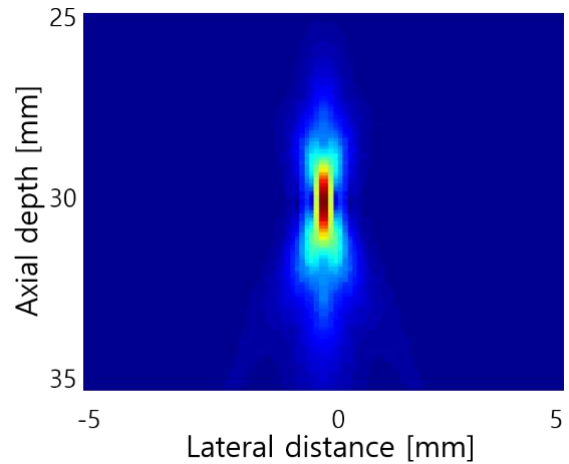


Fig. 5. Weighted DAS image with a 40 dB logarithmic compression.

IV. EXPERIMENT

We constructed an experimental setup for passive cavitation imaging to image ultrasound waves induced by bubble collapses due to focused ultrasound. The shock wave was generated using a device (model Shinewave-Sonic, HnT Medical, Republic of Korea), and the image data were acquired using an ultrasound research platform (model E-CUBE 12R, Alpinion, Republic of Korea) with a 5 MHz center frequency, 0.3 mm pitch, 128 element linear array transducer. Every other element was used on receive to make the effective pitch equal to 0.6 mm so that a total of 64 channels were used. The RF data were sampled at 40 MHz, stored in memory, and transferred to a PC, where they were interpolated by a factor of two to make the sampling rate equal to 80 MHz, and were processed to yield images.

In Fig. 6, (a) is the RF data due to single bubble collapse, (b) is the DAS image, (c) is the weighted DAS image, (d) is the RF data due two adjacent bubble collapse. For the case of a single bubble collapse, Figs. 6(b) and (c) are the DAS and weighted DAS images constructed using the RF data shown in Fig. 6(a), respectively. For the case of two adjacent bubble collapse, Figs. 6(e) and (f) are the DAS and weighted DAS images constructed using the RF data shown in Fig. 6(d), respectively. In the weighted images, the background noise tends to increase, but the resolution of cavitation bubbles increases. We can see that two cavitation bubbles are well resolved in the weighted two bubble collapse image. Since the cavitation size and presence are important, the background noise can be suppressed by thresholding in which signals whose levels are below a set value are removed.

V. CONCLUSION

Passive cavitation imaging with receive focusing based on the DAS method is disadvantageous in resolving small cavitation bubbles due to low resolution and large side lobe levels. To overcome this problem, the centroid and flatness were defined using the magnitude distribution in the channel data of the main and side lobe signals, and were applied to images in the form of weights. Since the centroid has a drawback of amplifying the surrounding noise, it was made to have a large value in the main lobe regions by combining with

the flatness. We confirmed by experiment that applying weights to single- and two-bubble collapse images substantially reduced side lobes and increased resolution.

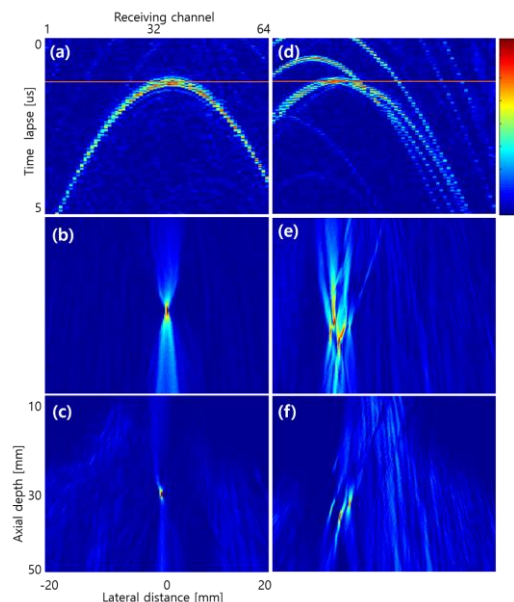


Fig. 6. Image construction: (a) RF echo from single-bubble collapse, (b) DAS image, (c) weighted single-bubble collapse image, (d) RF echo from two-bubble collapse, (e) DAS image, and (f) weighted two-bubble collapse image.

REFERENCES

- [1] V. A. Salgaonkar, S. Datta, C. K. Holland, and T. D. Mast, "Passive cavitation imaging with ultrasound arrays," *J. Acoust. Soc. Am.*, vol. 126, no. 6, pp. 3071–3083, Dec. 2009.
- [2] P. Boulos, F. Varray, A. Poizat, J. C. Bera, and C. Cachard, "Passive cavitation imaging using an open ultrasonic system and time reversal reconstruction," in *Proc. 22nd French Mechanics Congress*, 2015.
- [3] C. Coviello, R. J. Kozick, J. J. Choi, M. Gyöngy, J. Collin, C. Jensen, P. P. Smith, and C. C. Coussios, "Passive acoustic mapping using optimal beamforming for real-time monitoring of ultrasound therapy," in *Proc. Meetings on Acoustics*, 2013, pp. 1–7.
- [4] P. Boulos, F. Varray, A. Poizat, M. A. Kalkhoran, B. Gilles, J. C. Bera, and C. Cachard, "Passive cavitation imaging using different advanced beamforming methods," in *Proc. IEEE Ultrason. Symp.*, 2016.
- [5] J. H. Song, S. Cochran, P. Prentice, G. McLeod, and G. Corner, "Role of periodic shock waves in passive acoustic mapping of cavitation," in *Proc. IEEE Ultrason. Symp.*, 2016.
- [6] M. Gyöngy and C. C. Coussios, "Passive spatial mapping of inertial cavitation during HIFU exposure," *IEEE Trans. Biomedical Engineering*, vol. 57, no. 1, pp. 48–56, Jan. 2010.